Sustainable Food Technology

ROYAL SOCIETY OF CHEMISTRY

PAPER

View Article Online
View Journal

Cite this: DOI: 10.1039/d5fb00890e

Defatted coconut meal: a novel upcycled ingredient to improve anisotropic structuring and nutritional value of high-moisture meat analogues

A. A. Anoop,[ab] Anjali Sunil Ojha[a] and K. V. Ragavan *[ab]

Growing attention and efforts to create a sustainable food system for the burgeoning human population require a coordinated approach, including lowering the carbon footprint of food production, valorizing byproducts, and ensuring food and nutritional security. Diverse plant sources are being actively explored to replace animal- and monocrop-derived proteins in terms of their functionality and nutrition. Defatted coconut meal (DCM), a byproduct from the coconut industry containing significant amounts of proteins and dietary fiber, exhibits excellent hydration and interfacial properties. This study critically evaluated the potential of DCM to replace pea protein concentrate (PPC) in the range of 10–50% (w/w) for the production of high moisture meat analogues (HMMAs). Substitution with up to 20% DCM improved the fibrous alignment, matrix compactness, and muscle-like appearance. This correlated with higher disulfide bond formation, increased browning index, and elevated grafting degree relative to the control sample (100% PPC). However, DCM substitution beyond 30% led to structural fragmentation and reduced browning, indicating impaired network formation. The addition of transglutaminase to the 40–50% DCM formulation effectively restored the crosslinking density and structural integrity of the HMMA. These findings indicate that DCM can effectively substitute PPC in the formulation of HMMAs with improved textural and functional attributes. Moreover, DCM, being a rich source of dietary fiber, improves the nutritional value of HMMAs and qualifies as a food with a "rich source of dietary fibre" claim recommended by food regulations. This work highlights the role of DCM as a sustainable ingredient to improve the microstructure and nutritional profile of HMMAs.

Received 10th November 2025
Accepted 3rd March 2026

DOI: 10.1039/d5fb00890e

rsc.li/susfoodtech

Sustainability spotlight

This study evaluates the potential of coconut meal, a byproduct from the coconut industry, as an alternative to monocrop derived protein ingredients such as pea protein concentrate. Defatted coconut meal (DCM) was found to contain approximately 25% protein and 52% dietary fiber. Its functional properties in terms of hydration and interfacial properties were found to be excellent. Hence, pea protein concentrate was replaced with DCM for the production of high moisture meat analogs (HMMAs). DCM was found to improve the anisotropic fibrous nature of meat analogs and can be incorporated at levels up to 50% using transglutaminase. DCM also improved the nutritional attributes of meat analogs in terms of dietary fiber content. This research demonstrates a sustainable approach for upcycling food industry by-products for developing plant-based alternatives to conventional products. These findings contribute towards sustainable food production systems by developing functional ingredients from underutilized resources.

1. Introduction

The human population is growing rapidly and is expected to reach 9.7 billion by 2050.[1] This alarming increase exerts immense pressure on existing resources, leading to their over-exploitation, higher carbon emissions, and consequently contributing to climate change and global warming. Currently, food systems are responsible for roughly 30% of global anthropogenic greenhouse gas (GHG) emissions, with animal-derived foods accounting for nearly 60% of that share.[2,3] As a response to these issues, a shift towards sustainable and eco-friendly food alternatives is becoming increasingly necessary. The global vegan food market reflects this shift with a projected CAGR of 6.24% and is expected to reach 36.3 billion USD by the end of 2030.[4] Among various plant-based alternatives, HMMAs (high moisture meat analogues) play a critical role due to their ability to mimic the fibrous structure, chewiness, and juiciness of conventional meat products.[5] High-moisture extrusion cooking (HMEC) is an established and widely accepted technique for the production of HMMAs. This thermomechanical process uses heat, pressure, and shear, leading to protein denaturation, alignment, and subsequent formation of an

[a]CSIR-National Institute for Interdisciplinary Science and Technology, Thiruvananthapuram 695019, India. E-mail: vasanthragavan.niist@csir.res.in; Tel: +91 4712515443

[b]Academy of Scientific and Innovative Research (AcSIR), Ghaziabad 201002, India

anisotropic, fibrous structure that resembles muscle tissue. The success of HMMAs largely depends on the ability of the protein matrix to undergo controlled aggregation and alignment under shear flow, which are essential for developing a desirable meat-like texture.[5] Traditionally, soy, pea, and wheat proteins have served as the primary base materials for HMMAs. However, exclusive reliance on these sources is not entirely sustainable due to their environmental impact, cost, and limitations in replicating the complex fibrous structure of animal meat.[5] To achieve a more sustainable and circular food system, it is prudent to valorize agro-industrial byproducts that possess comparable nutritional and functional properties to conventional monocrop-derived plant proteins. One such underutilized byproduct is defatted coconut meal (DCM), obtained from coconut milk and virgin coconut oil extraction. In the context of HMMAs, the relevance of DCM lies in its techno-functional properties that influence extrusion behaviour and product structuring. DCM is rich in dietary fiber, constituting around 60%, with approximately 56% being insoluble and 4% soluble.[6] During HMEC, such fiber-rich materials can significantly influence water distribution, melt viscosity, and phase interactions, which are critical parameters governing fiber formation and textural development.[7–9]

However, incorporation of fiber-rich ingredients at high substitution levels may weaken protein network formation due to the reduced availability of reactive protein fractions, resulting in compromised structural integrity and poor anisotropic alignment.[10] Transglutaminase (TGase) is a widely used enzymatic crosslinker that enhances the texture and structural stability of plant-based meat analogues.[11] TGase catalyzes an acyl transfer reaction between the γ-carboxamide group of glutamine residues and the ε-amino group of lysine residues, resulting in the formation of covalent ε-(γ-glutamyl) lysine bonds.[12,13] This reaction strengthens the protein network by promoting intermolecular crosslinking, thereby improving matrix cohesiveness and fibrous structure development during extrusion.[11] Previous studies have demonstrated that TGase supplementation can enhance the structural organization and mechanical strength of extruded meat analogues by reinforcing the protein matrix, particularly in formulations containing polysaccharide-rich ingredients.[5] Therefore, TGase-assisted crosslinking represents a promising strategy to overcome the loss of structural integrity associated with high dietary fiber incorporation.

This study aims to investigate the effect of DCM substitution on the physicochemical, functional and microstructural properties of the extrudates. It is hypothesized that substituting part of the conventional protein base with DCM will yield extrudates that more closely mimic the structure and texture of animal meat, while simultaneously reducing production costs, improving nutritional value, and promoting valorization of the coconut industry by-products. Furthermore, TGase supplementation is expected to enhance covalent cross-linking and improve structural stability at higher DCM substitution levels, thereby supporting the development of fiber-rich HMMAs with improved texture. In doing so, this approach supports the broader goal of fostering a circular and sustainable food economy.

2. Materials and methods

2.1 Materials

Coconut meal was provided by Apex Coco and Solar Energy Ltd (Tamil Nadu, India). PPC was obtained from Urban Platter (Mumbai, India), and sunflower oil from a local market. OPA, sodium tetraborate, and Ellman's reagent were purchased from SRL (India), Merck (Germany), and HiMedia (India), respectively. ANS (8-anilinonaphthalene-1-sulfonic acid) was purchased from Sigma-Aldrich (USA) and transglutaminase from Bioven Ingredients (India). All experiments were conducted using distilled water.

2.2 Pre-treatment of coconut meal

The coconut meal was subjected to residual oil extraction, followed by milling and sieving to obtain a uniform particle size. The pretreated flour was termed defatted coconut meal (DCM) and was used as a substitute ingredient in high-moisture extrusion cooking.

2.2.1. Extraction of residual oil from coconut meal. Residual oil from coconut meal was extracted using a supercritical fluid extraction (SCFE) system (Model: SCFE/CTPL/002) manufactured by Cybernetik Technologies, India. A total of 500 g of coconut meal was loaded into a high-pressure-compatible polymeric mesh bag designed to withstand supercritical CO_2 conditions and placed into a 2-liter extraction vessel. The extraction was performed at a pressure of 350 bar and a temperature of 80 °C. Food-grade carbon dioxide (99.9% purity) was used as the supercritical solvent and was pumped at a constant flow rate of 62.19 g min^{-1}. The process was carried out in dynamic mode for a total duration of 3 h. The extracted oil was collected in a separator vessel by reducing the temperature and pressure to 25 °C and 50 bar, respectively.

2.2.3 Size reduction of DCM. DCM was milled using a heavy-duty grinder (Hakura, India) with a motor power of 2000 W and a motor speed of 25 000 rpm for 3 min. The milled flour was then fractionated based on particle size using an electromagnetic sieve shaker (ANM Industries, India) equipped with stainless steel (SS 316) sieves. The fraction with a particle size of 50 μm was collected and used for the preparation of meat analogues. This particle size was selected based on preliminary trials, as finer DCM particles ensured better dispersion and uniform blending with PPC, thereby minimizing fiber agglomeration and improving hydration during HMEC.

2.3 Proximate analysis of raw materials

The proximate composition of the raw materials used for meat analogue preparation was estimated using standard AOAC methods (AOAC, 2000).

2.3.1. Moisture content. The moisture content of the samples was measured following the AOAC method 934.01. About 2–3 g of each sample was placed in pre-weighed Petri dishes and dried in a hot air oven (Binder ED 115, France) at

105 °C for about 6 h or until a constant weight was achieved. Moisture percentage was calculated from the weight loss.

2.3.2. Oil content. Oil was extracted using the Soxhlet method as per the AOAC method 954.02. Around 5 g of sample was placed in a thimble and extracted with *n*-hexane for 6 h using a Soxhlet apparatus (Borosil Ltd, Mumbai, India) under continuous reflux.

2.3.3. Protein content. Protein was estimated using the micro-Kjeldahl method (AOAC 2001.11) with a Kjeltec™ 8400 analyzer (Denmark). The nitrogen content obtained was converted to protein using a conversion factor of 6.25.

2.3.4. Ash content. The ash content was measured following the AOAC method 942.05. About 5 g of sample was weighed into a porcelain crucible and incinerated in a muffle furnace at 550 °C for 6 h. The ash residue was then cooled and weighed to determine the total ash content.

2.3.5. Carbohydrate content. The carbohydrate content of the samples was calculated by difference, based on the measured values of moisture, protein, fat, and ash content.

2.4 Functional properties

2.4.1 Water absorption capacity and oil absorption capacity. The water absorption capacity (WAC) and oil absorption capacity (OAC) of the samples were determined according to the procedure described by Zahari *et al.* (2021). Briefly, 1 g of the sample was placed in a 15 mL centrifuge tube. Then, 10 mL of distilled water (for WAC) or 10 mL of sunflower oil (density: 0.92 g mL^{-1}) (for OAC) was added, and the mixture was vortexed for 2 min. The tubes were then centrifuged at 3000×*g* for 30 min. After centrifugation, the supernatant was carefully removed, and the pellet's weight was recorded.[14] WAC or OAC was calculated using the following equation:

$$\mathrm{WAC/OAC} = \frac{W_2 - W_1}{W_1} \quad (1)$$

where W_1 represents the initial sample weight (g) and W_2 is the weight of the pellet (g) after discarding the supernatant. The results are expressed as g g^{-1} for WAC and OAC.

2.4.2 Foaming capacity and foam stability. Foaming properties were measured following the procedure of Jakobson *et al.* (2023). For determining foaming capacity (FC), 0.2 g of the sample was weighed and transferred into a 50 mL centrifuge tube, followed by the addition of 20 mL distilled water. The mixture was frothed using a frother for 2 min.[15] FC was then calculated using eqn (2):

$$\mathrm{FC}(\%) = \frac{V_2 - V_1}{V_1} \quad (2)$$

where V_1 represents the initial sample volume before frothing (mL) and V_2 is the sample volume after frothing.

Foam stability (FS) was calculated by allowing the froth to stand undisturbed for 1 h after frothing. FS is calculated using eqn (3):

$$\mathrm{FS}(\%) = \frac{V_t}{V_0} \times 100 \quad (3)$$

where V_t is the foam volume (mL) after 1 h and V_0 is the initial foam volume measured immediately after frothing (mL).

2.4.3 Emulsion activity and emulsion stability. Emulsion activity (EA) and emulsion stability (ES) were measured according to the method reported by Jakobson *et al.* (2023). For EA, 0.24 g of the sample was mixed with 12 mL of distilled water and 12 mL of sunflower oil in a 50 mL centrifuge tube. The mixture was homogenized at 10 000 rpm for 1 min using a homogenizer (Daihan Scientific Co. Ltd, South Korea). The emulsion was then centrifuged at 1100×*g* for 5 min at 20 °C.[15] EA was calculated using eqn (4):

$$\mathrm{EA}(\%) = \frac{H_\mathrm{E}}{H_\mathrm{T}} \times 100 \quad (4)$$

where H_E is the height of the emulsion layer (cm) and H_T is the total height of the mixture (cm).

To determine ES, the emulsion was heated at 80 °C for 30 min in a water bath, and the height of the stable emulsion layer was recorded.

$$\mathrm{ES}(\%) = \frac{H_\mathrm{S}}{H_\mathrm{T}} \times 100 \quad (5)$$

where H_S is the height of the emulsified layer after heating and $H_{\mathrm{T\ is}}$ the total height of the mixture (cm).

2.4.4 Least gelation concentration. Sample dispersions ranging from 2% to 20% (w/v) were prepared in distilled water at 2% intervals. The pH of the samples was adjusted to 7 using 1 M NaOH or 1 N HCl. An aliquot of 5 mL was transferred to a clean glass test tube, heated at 100 °C for 1 h in a water bath, and then rapidly cooled with running tap water for 5 min. The tubes were then stored at 4 °C for 2 h in a refrigerator. The least gelation concentration (LGC) was defined as the minimum concentration at which the sample remained stationary when the tube was inverted.[16]

2.4.5 Bulk density. Bulk density (BD) was measured according to the method reported by Bhusari *et al.* (2014). In brief, 2 g of the sample was transferred into a 25 mL graduated measuring cylinder. The cylinder was then tapped 15 times from a height of 5 cm and the volume was recorded.[17] BD was calculated using eqn (6):

$$\mathrm{BD}\left(\mathrm{g\ mL^{-1}}\right) = \frac{\mathrm{Sample\ weight(g)}}{\mathrm{Volume\ of\ sample(mL)}} \quad (6)$$

2.5 High moisture extrusion cooking

All extrusion experiments were performed using a laboratory-scale twin-screw extruder (Basic Technology Private Ltd, Kolkata, India), equipped with a custom-designed cooling die developed at CSIR-NIIST (Thiruvananthapuram, India) in collaboration with Stonehat Technologies (Coimbatore, India). The extruder consisted of a single heated barrel zone, and the barrel temperature was maintained at 120 °C throughout the process. Extrusion parameters were set based on preliminary optimization trials: feed moisture content was maintained at 55.56% (a solid to water ratio of 1 : 1.25), screw speed at 360 rpm, feeder speed at 6 rpm equivalent to a feeding rate of

2.25–2.5 kg h^{-1}, and torque was monitored during extrusion and maintained at approximately 4 N m. The average residence time of the raw material inside the extruder was in the range of 4–6 min. The cooling die featured three distinct zones with decreasing temperature gradients: 19 °C, 15 °C, and 11 °C, starting from the extruder end. This facilitated proper texturization and stabilization of the extrudates.

A total of seven extrusion trials were conducted to evaluate the effect of DCM and transglutaminase on the fibrous structure formation in meat analogues. The first trial (control) used 100% pea protein and in the subsequent trials, the pea protein was gradually substituted with DCM at different ratios: 10% DCM + 90% pea protein (Trial 2), 20% DCM + 80% pea protein (Trial 3), 30% DCM + 70% pea protein (Trial 4), and 40% DCM + 60% pea protein (Trial 5). To improve fibrous texture, transglutaminase (0.25% w/w) was incorporated into two additional trials: 40% DCM + 60% pea protein + 0.25% transglutaminase (Trial 6) and 50% DCM + 50% pea protein + 0.25% transglutaminase (Trial 7). All dry ingredients were mixed thoroughly and kept in plastic bags at 4 °C for 1 h to condition the mixture. For TGase-containing samples (Trial 6 and Trial 7), the hydrated mixture was incubated in an incubator at 50 °C for 1 h prior to extrusion to facilitate enzymatic crosslinking. TGase activation was achieved during this pre-extrusion incubation step. The enzyme was subsequently inactivated upon entering the high-temperature melting zone.[18]

2.6 Colour analysis

The colour parameters of the meat analogues were measured using a HunterLab Colorimeter (ColorFlex EZ, Virginia, USA) and expressed as CIE L^* a^* b^*. The instrument employed directional 45° annular illumination and simulated daylight conditions using the standard D65 illuminant, which was achieved *via* a pulsed xenon light source. A view diameter of 25.4 mm was used for measurements. Prior to analysis, the device was calibrated using a standard white tile having L^*, a^*, and b^* values of 98.014, −0.032 and 1.459, respectively. Colour measurements were performed on the surface of intact extrudates (without grinding). The extrudates were cut into rectangular blocks (4 cm × 4 cm), and measurements were recorded from the flat surface. Each sample was analyzed at least three times to ensure reproducibility, and the mean L, a, and b values were reported. The colour difference (ΔE) of meat analogues was calculated using eqn (7), with respect to the control sample (100% pea), to enable direct comparison among formulations.[19] Whiteness Index (WI) and Browning Index (BI) were calculated using eqn (8) and (9), respectively.[20]

$$\Delta E = \sqrt{\left(L_{\text{sample}} - L_{\text{standard}^*}\right)^2 + \left(A_{\text{sample}} - A_{\text{standard}^*}\right)^2 + \left(B_{\text{sample}} - B_{\text{standard}^*}\right)^2} \quad (7)$$

$$\text{WI} = 100 - \sqrt{(100 - L^*)^2 + a^{*2} + b^{*2}} \quad (8)$$

$$\text{BI} = \left(\frac{100}{0.17}\right) \times \left(\frac{a + 1.75 \times L^*}{5.645 \times L^* + a^* - 3.012 \times b^*} - 0.31\right) \quad (9)$$

2.7 Total dietary fiber

Total dietary fibre content was determined using the Megazyme Integrated Total Dietary Fibre Assay Kit (Megazyme International, Bray, Ireland) following AOAC Methods 2009.01 and 2011.25.[21,22] Approximately 1 g of sample was enzymatically digested with heat-stable α-amylase, protease, and amyloglucosidase, followed by ethanol precipitation of soluble components. The residue was filtered, dried, and corrected for protein and ash contents. The results are expressed as a percentage of total dietary fibre on a dry weight basis.

2.8 FTIR

FTIR analysis of the meat analogue samples was performed using an attenuated total reflectance-Fourier transform infrared (ATR-FTIR) spectrometer (Bruker Alpha-T, Germany). Measurements were obtained using a diamond ATR crystal over a wavenumber range of 400–4000 cm^{-1} with a spectral resolution of 4 cm^{-1}. A total of 32 background scans were averaged and used to correct the sample spectra. The ATR diamond crystal was cleaned using isopropanol after every sample.

2.9 Surface hydrophobicity

The surface hydrophobicity (H_0) of the HMMA samples was assessed using 8-anilinonaphthalene-1-sulfonic acid (ANS) following the protocol described in ref. 23 with slight modifications. The samples were dispersed in 10 mM phosphate buffer (pH 7.0), vortexed for 2 min, and then centrifuged at 10 000 g for 10 min. The resulting supernatant was diluted to protein concentrations ranging from 0.05 to 0.5 mg mL^{-1}. To 4 mL of diluted protein solution, 20 μL of 8 mM ANS was added and the mixture was incubated in the dark for 15 min. Fluorescence intensity was measured using a fluorescence spectrophotometer (Synergy H1 Gen5 3.05) (BioTek Instruments, USA) with an excitation wavelength of 370 nm and an emission wavelength of 470 nm. A graph was plotted with fluorescence intensity against protein concentration, and the slope of the linear region was taken as the hydrophobicity index.

2.10 Degree of grafting

The degree of grafting (DG) was assessed using the *O*-phthalaldehyde (OPA) reagent-based method,[24] with some modifications. Briefly, 250 mg of HMMA sample was dissolved in 20 mL of distilled water, vortexed for 2 min, and then centrifuged at 5000 g for 5 min. An aliquot of 200 μL from the resulting

supernatant was mixed with 4 mL of freshly prepared OPA reagent and incubated in a water bath at 90 °C for 5 min. After incubation, absorbance was measured at 340 nm using a UV-vis spectrophotometer (Infinite M200 PRO, Tecan, Switzerland). Distilled water mixed with the OPA reagent (without sample) was used as the reagent blank. The DG was measured using eqn (10) and expressed as a percentage.

$$\mathrm{DG} = \frac{A_0 - A_1}{A_0} \times 100\% \quad (10)$$

where A_0 represents the absorbance of the control extrudate (100% pea protein HMMA) and A_1 represents the absorbance of the corresponding DCM substituted extrudates.

2.11 Determination of free sulfhydryl groups and disulfide bonds

The quantification of free and total sulfhydryl (SH) groups in HMMA samples was performed following the method described by Xiao *et al.* (2025).[25] For sample preparation, 75 mg of HMMA was dispersed in 10 mL of Tris–Gly–Urea buffer (86 mM Tris, 90 mM glycine, 4 mM EDTA, and 8 M urea) and kept under continuous shaking overnight.

To determine the free SH content, 1 mL of the extracted sample was mixed with 4 mL of Tris–Gly buffer and 50 μL of Ellman's reagent (4 mg mL^{-1}). The mixture was incubated in the dark for 15 min, followed by centrifugation at 8000*g* for 8 min. The absorbance of the supernatant was measured at 412 nm using a UV-vis microplate reader (Infinite M200 PRO, Tecan, Switzerland).

To estimate the total sulfhydryl content, 1 mL of the sample was mixed with 4 mL of Tris–Gly buffer and 0.05 mL of β-mercaptoethanol solution, followed by incubation for 1 h at room temperature (25 °C) with gentle shaking. The well dispersed mixture was then treated with 10 mL of 12% trichloroacetic acid (TCA) and centrifuged at 8000*g* for 8 min to separate the protein in the form of a pellet. The pellet was washed and redispersed in 10 mL Tris–Gly buffer. To the dispersion, 40 μL of Ellman's reagent was added and incubated in the dark for 15 min. After incubation, the solution was centrifuged at 8000*g* for 8 min, and the absorbance of the supernatant was recorded at 412 nm.[25]

The concentrations of free sulfhydryl and disulfide bonds were calculated using the following equations, respectively:

$$\mathrm{SH\ content}\left(\mu\mathrm{M\ g^{-1}}\right) = \frac{73.53 \times A412 \times D}{C} \quad (11)$$

$$\mathrm{Disulfide\ bonds\ content}\left(\mu\mathrm{M\ g^{-1}}\right) = \frac{(\mathrm{Toatl\ SH\ content} - \mathrm{Free\ SH\ content})}{2} \quad (12)$$

where $A412$ represents the absorbance measured at 412 nm, D denotes the dilution factor (5 for free sulfhydryl content and 10 for total sulfhydryl content), and C is the sample concentration expressed in mg mL^{-1}.

2.12 Scanning electron microscopy

The microstructure of meat analogue samples was examined using a scanning electron microscope (Zeiss EVO-60, Germany). The samples were cut into small pieces (5 × 5 × 2 mm) and freeze-dried. The dried samples were then sputter-coated with gold, and the microstructures were recorded under high-vacuum conditions at magnifications of 300×, 1000×, and 1500× to evaluate surface characteristics.

2.13 Data analysis

Data are expressed as mean ± standard deviation ($n = 3$). Statistical significance was determined using one-way ANOVA followed by Tukey's HSD test ($p < 0.05$) using the Astatsa online calculator. Different superscript letters indicate significant differences between means.

3. Results and discussion

3.1 Preprocessing of coconut meal

To improve the suitability of coconut meal for meat analogue production, residual oil (32%) was removed using supercritical carbon dioxide extraction (SCFE), yielding defatted coconut meal (DCM) with a fat content of around 1%. This defatting process led to a significant increase in protein content from 13.91% in coconut meal to 24.68% in DCM (Table 1). This protein content is comparable to previously reported values for coconut meal/cake (4–25%), which vary depending on the processing and defatting methods used.[26–28] The relatively higher protein content observed in the present study may be attributed to the efficient removal of residual oil by SCFE, which concentrates the non-fat components, particularly proteins, in the DCM. In addition, carbohydrate content increased from 42.5% to 63.3%, indicating a compositional enrichment of non-fat nutrients due to the oil extraction. Post-extraction, the DCM was obtained as flakes with a relatively larger particle size; it was milled and sieved to a uniform particle size of 50 μm to ensure homogeneity during blending.

3.2 Functional properties of raw materials

Functional properties can be broadly classified into two groups: hydration properties (WAC, OAC, and gelation) and surface active properties (emulsification and foaming).[29,30] WAC refers to the amount of water absorbed per gram of sample and depends on the particle size, carbohydrate composition, and

Table 1 Proximate analysis of PPC, coconut flour, and DCM[a]

	PPC	Coconut meal	DCM
Moisture %	6.3 ± 0.69^{b}	7.52 ± 0.13^{a}	5.91 ± 0.36^{b}
Ash %	3.01 ± 0.02^{c}	4.03 ± 0.17^{b}	4.9 ± 0.1^{a}
Protein %	80.50 ± 1.5^{a}	13.91 ± 0.04^{c}	24.68 ± 0.3^{b}
Fat %	0.08 ± 0.01^{c}	32.04 ± 0.37^{a}	1.21 ± 0.09^{b}
Carbohydrate %	10.1^{c}	42.5^{b}	63.3^{a}

[a] Values are expressed as mean ± standard deviation ($n = 3$). Different superscript letters (a–c) within the same row indicate statistically significant differences between means ($p < 0.05$).

the availability of polar amino acids.[16,31] Pea proteins are reported to have a WAC of approximately 4.0 g g^{-1}, and the pea protein used in this study has a WAC of 3.66 ± 0.36.[32] DCM was found to have a WAC of 3.15 ± 0.36 g g^{-1} (Fig. 1a), which can be attributed to the presence of water-soluble galactomannan and polar amino acids.[6] Overall, both ingredients exhibited relatively high WAC values, suggesting strong hydration capacity.

Another critical parameter in HMMA formulation is the OAC, which reflects the oil absorption potential of the ingredients. Pea protein exhibited an OAC of 1.21 ± 0.12 g g^{-1}, which was consistent with earlier findings,[33] whereas DCM showed a significantly higher OAC of 2.52 g g^{-1} (Fig. 1b). This superior OAC is likely due to DCM's high content of insoluble amphiphilic fiber and its porous microstructure, which remains intact following SCFE of coconut meal.[6,34] Such amphiphilic fibers are known to enhance the interactions between polymers, especially denatured proteins during high-moisture extrusion, thereby contributing to the formation of cohesive and structured protein matrices.[35]

In terms of surface-active functionality, DCM exhibited superior emulsifying and foaming properties compared to pea protein. The emulsifying capacity of DCM was found to be 10.83% (Fig. 1c), significantly higher than that of pea protein (1.28%). This can be attributed to the amphiphilic proteins and polysaccharides present in coconut meal, which contribute to reducing interfacial tension and stabilizing emulsions.[34] For comparison, lean meat proteins like myofibrillar proteins also show strong emulsifying capacity due to their ability to form elastic gels that encapsulate fat and water. This suggests that DCM could serve as a suitable ingredient for HMMA formulations, as it has a significantly higher emulsifying capacity when compared to pea protein.[36] DCM also demonstrated an emulsion stability of 5.17% (Fig. 1d), much higher than that of pea protein (1.25%), indicating that the gels formed with DCM are more stable and less prone to phase separation. These findings align with earlier reports that dietary fibers from apple and citrus enhance the stability of meat emulsions by promoting uniform texture and preventing phase separation.[37,38]

Regarding foaming properties, DCM exhibited a foaming capacity of 31% (Fig. 1e), which is substantially higher than that of pea protein (13%). Although pea protein demonstrated slightly higher foam stability (Fig. 1f), the higher initial foaming capacity of DCM makes it valuable for improving the aeration and textural lightness of meat analogues.[39] In terms of gelling ability, both DCM and pea protein showed a comparable gelation capacity of 12% (Fig. 1h), suggesting that DCM can provide similar textural firmness and network formation in high-moisture meat analogue systems. Finally, DCM was characterized by a lower bulk density (0.30 g mL^{-1}) (Fig. 1g) compared to pea protein (0.52 g mL^{-1}), which is likely due to SCFE of residual oil, resulting in a more porous structure.[34] Overall, the findings suggest that the functionality of DCM complements that of pea protein, and it can be effectively incorporated into HMMA formulations without compromising extrudate quality.

3.3 High moisture extrusion cooking

HMEC is a thermomechanical process that applies controlled heat, shear, and pressure to denature plant proteins and align

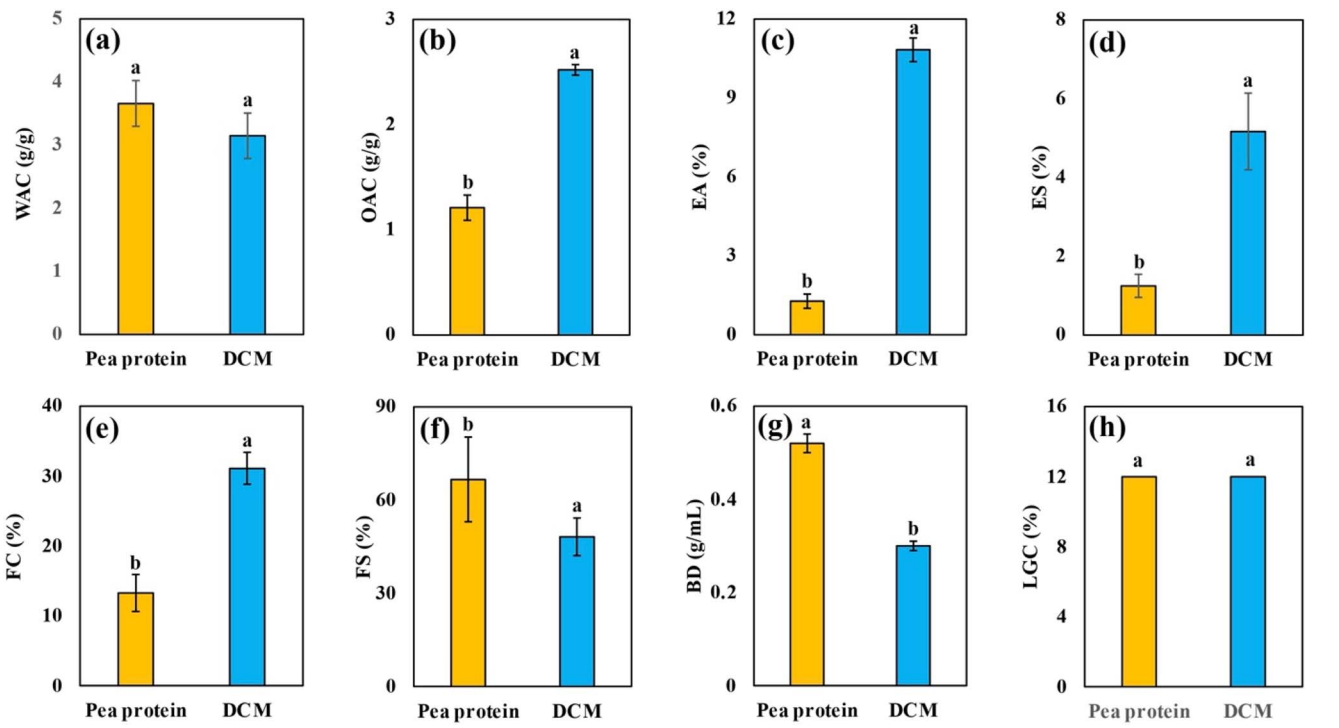

Fig. 1 Comparison of functional properties between pea protein and DCM: (a) water absorption capacity (WAC), (b) oil absorption capacity (OAC), (c) emulsion activity (EA), (d) emulsion stability (ES), (e) foaming capacity (FC), (f) foaming stability (FS), (g) bulk density (BD), and (h) least gelation concentration (LGC). Values are expressed as mean ± SD ($n = 3$). Different superscript letters indicate significant differences ($p < 0.05$).

them into fibrous structures resembling animal muscle. The process involves mixing, melting, and texturizing stages, followed by cooling to stabilize the anisotropic structure.[5,40] A schematic representation of the HMEC process and cooling die system is shown in Fig. 2, illustrating the key zones and temperature gradients that facilitate structure formation.

3.4 Color analysis

Color is a critical quality attribute influencing the sensory perception and consumer acceptability of meat analogues. The colour of the extrudates is influenced by the intrinsic colour of raw materials and browning reactions such as the Maillard reaction and caramelization occurring during extrusion.[19] DCM exhibited a markedly lighter colour ($L^* = 90.03 \pm 0.11$, $a^* = 1.56 \pm 0.03$, and $b^* = 11.78 \pm 0.14$) compared to PPC, which showed values of $L^* = 81.27 \pm 0.05$, $a^* = 3.41 \pm 0.01$, and $b^* = 27.39 \pm 0.08$. The higher L^* and lower a^* and b^* values of DCM indicate a lighter, less reddish, and less yellow appearance relative to PPC. The results of extrusion trials indicate a linear increase in lightness (L^*) values with increasing levels of DCM substitution (Table 2). The L^* value increased from 45.68 ± 2.8 for the control meat analogue to 59.43 ± 1.12 for the 40 DCM substituted sample. This increase can be attributed to the inherently higher lightness of DCM, which has an L^* value of around 90, compared to pea protein ($L^* \approx 81$). In contrast, the a^* and b^* values remained relatively stable across all DCM

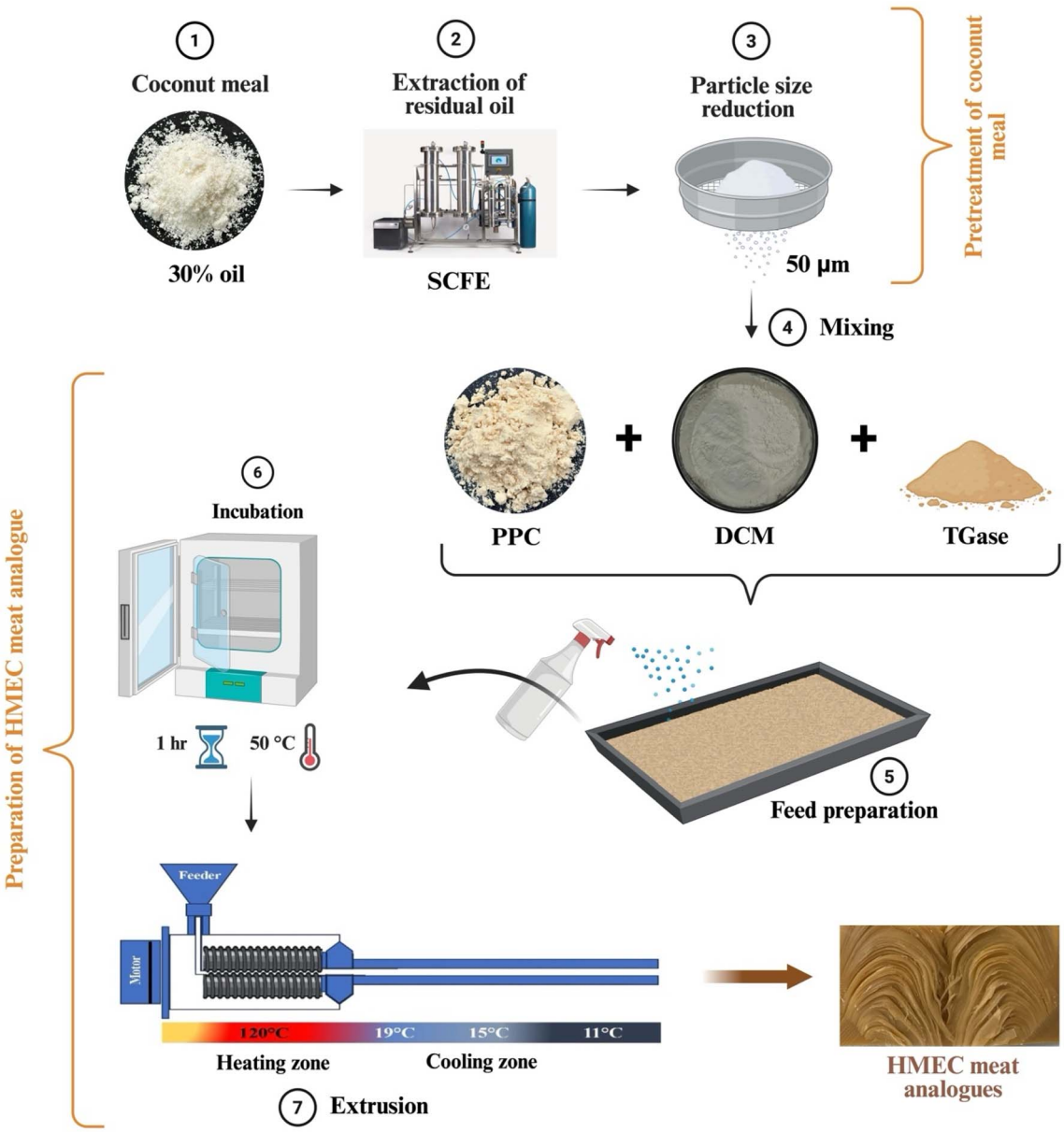

Fig. 2 Process flowchart for the preparation of HMMAs using DCM and pea protein. Residual oil was removed from coconut meal using SCFE, followed by pulverization and sieving (50 µm). DCM was blended with pea protein and TGase, and moisture was adjusted to 55.56%. TGase-containing blends were incubated at 50 °C for 1 h prior to extrusion.

Table 2 Colour parameters of meat analogues[a]

Trial	Samples	L^*	a^*	b^*	ΔE	WI	BI
1	100% PPC	45.68 ± 2.8^{b}	6.6 ± 0.52^{a}	23.1 ± 0.66^{ab}		40.59 ± 2.53^{c}	79.33 ± 6.71^{a}
2	10% DCM	44.96 ± 2.34^{b}	5.86 ± 0.53^{a}	22.41 ± 1.1^{ab}	2.35 ± 1.9^{a}	40.26 ± 1.89^{c}	76.57 ± 4.16^{ab}
3	20% DCM	45.62 ± 1.01^{b}	5.45 ± 1^{a}	22.81 ± 2.01^{b}	2.7 ± 0.39^{a}	40.84 ± 1.21^{c}	76.25 ± 8.69^{ab}
4	30% DCM	54.53 ± 0.65^{ab}	5.63 ± 0.11^{a}	24.02 ± 0.37^{ab}	8.96 ± 0.69^{b}	49.24 ± 0.78^{b}	64.21 ± 1.02^{ab}
5	40% DCM	59.43 ± 1.12^{a}	5.82 ± 0.14^{a}	24.95 ± 0.63^{a}	13.91 ± 1.12^{d}	54.07 ± 1.25^{a}	60.45 ± 2.92^{b}
6	40% DCM + 0.25% Tgase	58.62 ± 0.52^{a}	5.96 ± 0.13^{a}	24.15 ± 0.68^{ab}	13.02 ± 0.68^{d}	53.48 ± 0.69^{a}	59.39 ± 1.69^{b}
7	50% DCM + 0.25% Tgase	56.82 ± 0.79^{a}	5.74 ± 0.23^{a}	24.28 ± 0.55^{ab}	11.34 ± 0.77^{c}	50.41 ± 0.55^{ab}	59.92 ± 1.6^{b}

[a] Values are expressed as mean ± standard deviation ($n = 3$). Different superscript letters (a–d) within a column indicate statistically significant differences between means ($p < 0.05$).

substitutions, indicating that redness and yellowness were not significantly altered by DCM addition. The addition of TGase resulted in a slight reduction in L^* values for both the 40% and 50% DCM samples. The darker appearance of the sample may be due to the crosslinked protein, which enhances the light absorption due to the formation of compact protein networks.[41,42]

The total colour difference (ΔE), calculated with respect to the control sample, increased significantly with increasing DCM substitution. Samples with 10% and 20% DCM showed low ΔE values (2.35 ± 1.9 and 2.7 ± 0.39, respectively), indicating a minimal perceptible difference from the control. However, higher substitution levels resulted in a marked increase in ΔE, with values of 8.96 ± 0.69 (30% DCM), 13.91 ± 1.12 (40% DCM), and 11.34 ± 0.77 (50% DCM + TGase), indicating clearly perceptible color differences. The addition of TGase slightly reduced ΔE compared to 40% DCM, suggesting a minor stabilizing effect on colour development. The brown colour of the meat analogue is primarily developed through Maillard reactions and caramelization during the extrusion process.[43] The Browning Index (BI) remained high and relatively constant up to 20% DCM substitution (76.57–76.25), suggesting that the Maillard reaction occurred efficiently in these formulations. A notable decline in BI was observed beyond 30% substitution, with values dropping to 64.21 for 30% DCM and further to 60.45 for 40% DCM. This reduction is likely due to the limited availability of reactive carbonyl and amino groups required for the Maillard reaction, as well as the dilution effect caused by the predominantly bright DCM, which diminishes the browning intensity and hinders the extent of the Maillard reaction. However, the addition of TGase maintained constant BI values, suggesting that TGase indirectly enhances the Maillard reaction, a phenomenon also reported in previous studies[20]

The whiteness index (WI) remained relatively constant (~40) up to 20% DCM substitution, indicating good blending and intercalation with pea protein. Beyond 20%, the WI increased significantly, reaching 54.07 at 40% DCM, reflecting the increased presence of DCM. With TGase addition, the WI shows reduction, which suggests enhanced crosslinking between DCM and pea protein, resulting in a more uniform matrix with less visible whiteness. In short, DCM incorporation significantly influenced the color properties of meat analogues by increasing the lightness. Moderate substitution (up to 20%) maintained favorable Maillard browning, while higher levels reduced browning intensity.

3.5 Total dietary fiber content

Dietary fiber consists of non-starch polysaccharides and lignin that are resistant to digestion in the small intestine and are subsequently fermented by microbiota in the colon.[44] Previous studies have reported that the dietary fiber present in DCM is fermentable in colon, where it is converted into short-chain fatty acids mainly acetate, propionate, and butyrate, which help lower the glycemic index, serum cholesterol, LDL cholesterol, and triglyceride levels.[45] In the present study, DCM exhibited a total dietary fiber (TDF) content of 52.29%, consistent with earlier reports indicating TDF values ranging from 40% to 63.25% in coconut flour. The variation in fiber content among studies is mainly due to the difference in the maturity stages of coconuts and the quality of the raw material, which influence the amount of residual fat remaining in the coconut flour.[34,46–48] Table 3 presents the TDF content of HMMA samples prepared with increasing DCM substitution. The high dietary fiber content of DCM enables it to act as a binder with high water and oil holding capacities, which contribute to improved fibrous alignment and structural stability of the protein matrix during extrusion.[46,49]

The 10% DCM substituted HMMA contained 2.33% dietary fiber (5.25 ± 0.21% on a dry basis). According to the FSSAI, a solid food product containing at least 3% TDF can be labeled as a source of dietary fiber, while products with TDF ≥ 6% can be labeled as high in dietary fiber.[50] The 20% DCM substituted HMMA, with a dietary fiber content of 4.59% (10.32 ± 0.14% on

Table 3 TDF content of HMMA samples[a]

Trial	Samples	TDF (dry basis)
1	100% PPC	0.89 ± 0.03^{a}
2	10% DCM	5.25 ± 0.21^{b}
3	20% DCM	10.32 ± 0.14^{c}
4	30% DCM	15.3 ± 0.27^{d}
5	40% DCM	20.73 ± 0.47^{e}
6	40% DCM + 0.25% Tgase	20.42 ± 0.32^{f}
7	50% DCM + 0.25% Tgase	26.23 ± 0.24^{g}

[a] Values are expressed as mean ± standard deviation ($n = 3$). Different superscript letters indicate significant differences ($p < 0.05$).

a dry basis), qualifies as a source of dietary fiber. Meanwhile, the 30% DCM-substituted HMMA, with 6.8% fiber (15.3 ± 0.27% on a dry basis), qualifies as rich in dietary fiber as per FSSAI standards. The formulations containing more than 30% DCM substitution, therefore, meet the criteria for being high in dietary fiber. Interestingly, improved fibrous alignment was observed up to 20% DCM substitution, suggesting that moderate fiber enrichment supports matrix structuring during HMEC. SEM micrographs further supported this observation, showing a more compact and aligned fibrillar morphology at lower substitution levels, whereas higher DCM incorporation resulted in micro-tears and fragmented structures. This indicates that although dietary fiber contributes to water binding and physical reinforcement, excessive fiber may dilute the protein fraction required for continuous network formation, thereby reducing structural integrity. Furthermore, the results indicated that HMEC had little to no effect on the total dietary fiber content, as no significant reduction was observed post-extrusion, which supports previous reports that extrusion processing minimally affects TDF content.[51,52]

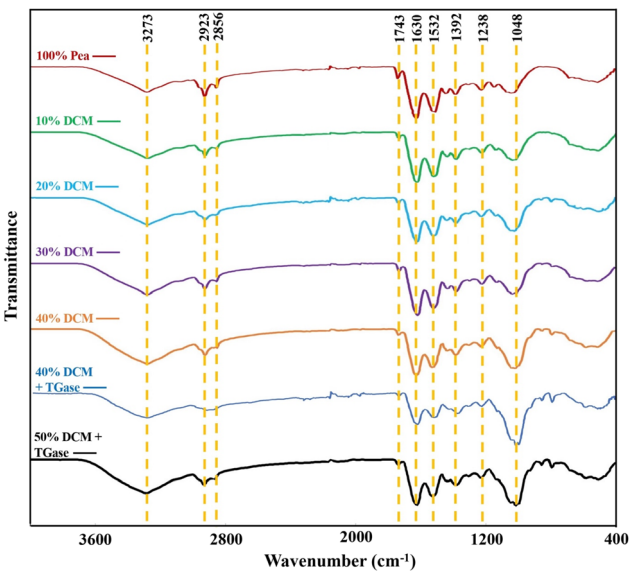

Fig. 3 FTIR spectra of HMMAs with varying levels of DCM.

3.6 FTIR

FTIR spectroscopy was used to examine the molecular interactions between biopolymers in HMMA (Fig. 3), and the corresponding wavenumbers, vibration types, and functional group assignments are summarized in Table 4. A broad absorption band between 3200 and 3600 cm^{-1} corresponds to O–H and N–H stretching vibrations, characteristic of hydroxyl groups in polysaccharides and amide groups in proteins, respectively.[53,54] The broad peak around 3273 cm^{-1} indicates overlapping contributions from these components, and its increased intensity with DCM addition suggests enhanced hydrogen bonding interactions in the HMMA matrix, likely due to the high fibre content of DCM.[54–56] Weak absorption peaks in the 2800–3000 cm^{-1} range are associated with the C–H stretching vibrations of aliphatic CH_2 and CH_3 groups, primarily from polysaccharides, with minor contributions from protein side chains.[56] The weak absorption band at 1743 cm^{-1} corresponds to the C=O stretching vibration of the carbonyl ester groups, indicative of lipid associated groups in biological materials. This band likely arises from the minor amount of triglycerides present in DCM and PPC.[57,58]

The Amide II band around 1532 cm^{-1} corresponds to the C–N stretching coupled with N–H bending, representing the protein's secondary structural features.[59,60] The absorption band at 1238 cm^{-1} corresponds to the N–H bending and C–N stretching vibrations characteristic of the amide I band.[61,62] The peak observed at 1630 cm^{-1} corresponds to the C=O stretching of the amide III band.[59] The absorption peak at 1392 cm^{-1} corresponds to the C–H bending vibrations of alkanes, associated with aliphatic groups present in both proteins and polysaccharides.[63] The peak observed at 1048 cm^{-1} corresponds to the C–O stretching vibrations of carbohydrates. Similar results have been reported by Wang *et al.* (2024), who observed structural changes in HMMAs with the incorporation of starch.[56] This peak was less intense in the 100% pea-based HMMA, reflecting the low carbohydrate content of pea protein concentrates. A gradual increase in peak intensity with higher DCM substitution indicates the higher fibre content contributed by DCM.[53]

Overall, FTIR spectra demonstrate the coexistence of characteristic functional groups of proteins, polysaccharides, and lipids in the HMMA matrix. The increased OH and C–O band intensities and broader hydrogen-bond peaks indicate effective

Table 4 Characteristic FTIR spectra for the corresponding vibration types and functional groups

Wavenumber (cm^{-1})	Functional group	Vibration type	Assignment	Reference
3200–3600	N–H/O–H	Stretching	Polysaccharides/proteins	53, and 54
2800–3000	C–H	Stretching	Polysaccharides/proteins	56
1743	C=O	Stretching	Triglycerides	57, and 58
1630–1670	C=O	Stretching	Amide III	59, and 60
1510–1580	C–N/N–H	Stretching/bending	Amide II	59, and 60
1392	C–H	Bending	Alkanes	63
1238	C–N/N–H	Stretching/bending	Amide III	61, and 62
980–1050	C–O	Stretching	Polysaccharides	53

incorporation of DCM and stronger protein–fiber interactions, improving the structural stability of the extruded product.

3.7 Surface hydrophobicity (H_0)

Surface hydrophobicity (H_0) can be used as an indicator of protein denaturation during extrusion, reflecting processes such as protein oxidation and aggregation.[64] It is measured using an ANS probe, which binds to the hydrophobic regions of protein in the layer that become exposed during protein unfolding.[65] As shown in Fig. 4, the control sample (100% pea protein) exhibited an H_0 value of 3418.5, while the 10% DCM sample showed the highest H_0 value of 3813.5, indicating enhanced surface exposure of hydrophobic residues. This increase can be attributed to hydrogen bonding between pea protein and DCM, which weakens intramolecular hydrophobic interactions and enhances the accessibility of hydrophobic domains to the ANS probe. Similar trends were observed in previous studies, where the incorporation of polysaccharides such as curdlan increased hydrophobicity by modifying protein interactions.[24]

However, as the DCM substitution increased from 20% to 40%, H_0 values decreased progressively (3164, 2432, and 1533, respectively). This decline may result from the formation of protein aggregates that shield hydrophobic sites or from the dilution effect caused by increasing DCM content, which has a lower protein concentration than pea protein.[66] Interestingly, the addition of TGase at 40% DCM led to an increase in hydrophobicity. This suggests that TGase-induced crosslinking may promote partial unfolding or rearrangement of protein structures, thereby exposing hidden hydrophobic regions. This is consistent with previous studies that TGase facilitates the formation of extended protein networks through acyl transfer reactions.[20] In contrast, the 50% DCM extrudates exhibited a sharp decline in hydrophobicity. This reduction is likely due to a higher amount of DCM in the formulation, which impairs protein unfolding and crosslinking due to the low protein content and high fiber matrix. Additionally, steric hindrance or interference from fiber-rich DCM may obstruct ANS probe binding, thereby reducing fluorescence intensity.[7] Overall, moderate DCM incorporation enhanced the surface hydrophobicity of the extrudate by promoting its interaction with PPC, while excessive substitution reduced H_0 values due to limited protein availability and fiber interference. TGase addition mitigated this effect by restoring hydrophobic exposure through enzymatic crosslinking.

3.8 Degree of grafting

The degree of grafting (DG) indicates the reduction in free amino group content of the extrudates, which indicates the extent of protein–protein or protein–polysaccharide crosslinking, particularly between pea protein and DCM. During extrusion, proteins are subjected to high temperature, pressure, and shear, leading to protein unfolding and increased reactivity of amino acid residues. These exposed groups can form intermolecular interactions with DCM proteins and polysaccharides, contributing to the formation of a fibrous texture.[9,67] As shown in Fig. 5, the DG values increased progressively with higher DCM substitution levels. Specifically, DG ranged from 4.84% (10% DCM) to a maximum of 17.15% (50% DCM + TGase), indicating enhanced protein modification and interaction with increasing DCM levels. Previous studies have reported that the addition of polysaccharides such as curdlan and β-glucan increased DG due to stronger binding between unfolded proteins and carbohydrates.[9,24] In this study, the observed DG increase can be attributed to the higher availability of reactive glutamine residues from DCM proteins, which facilitate TGase-mediated crosslinking.

The addition of TGase further increased the DG values, with values increasing from 9.47% (40% DCM) to 16.26% (40% DCM + TGase) and 17.15% (50% DCM + TGase). DCM contains approximately 25% glutamic acid, which serves as a precursor for glutamine residues—the acyl donor in TGase-catalyzed reactions.[68] These glutamine residues enable the formation of ε-(γ-glutamyl)lysine bonds by crosslinking with lysine residues from pea protein.[69] Hence, the high glutamic acid content of DCM might contribute to a greater pool of available crosslinking sites, enhancing the protein network. In conclusion,

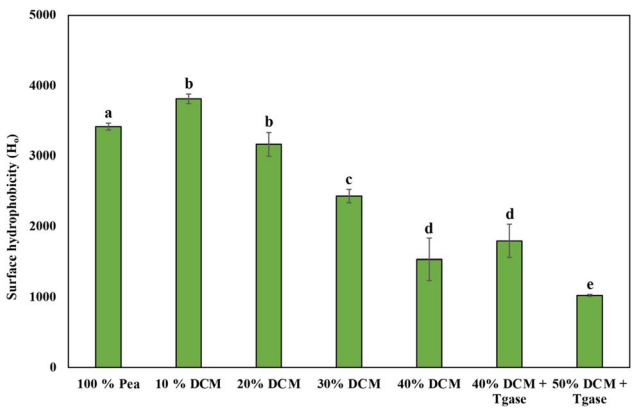

Fig. 4 Surface hydrophobicity (H_0) of extrudates formulated with different ratios of DCM and pea protein, including trials with 0.25% (w/w) TGase. Values are presented as mean ± SD, and different superscript letters indicate significant differences ($p < 0.05$).

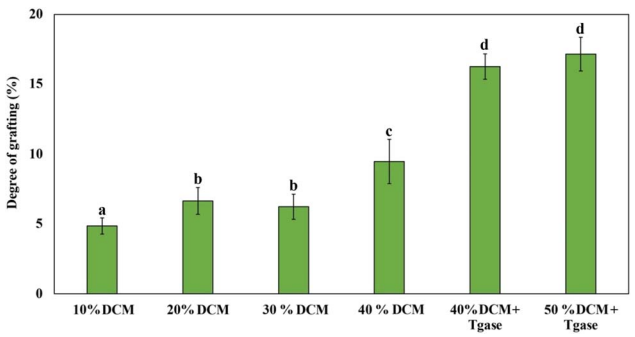

Fig. 5 Degree of grafting (%) of extrudates formulated with varying levels of DCM and pea protein, including trials with 0.25% (w/w) TGase, as determined by OPA assay. Values are presented as mean ± SD, and different superscript letters indicate significant differences ($p < 0.05$).

these results demonstrate that DCM is capable of effectively interacting and forming covalent linkages with pea protein, making it a promising functional substituent for use in HMMAs.

3.9 Free sulfhydryl groups and disulfide bonds

The content of free sulfhydryl groups is a key indicator of protein unfolding and potential disulfide bond formation during HMEC. As shown in Fig. 6a, the raw material exhibited significantly higher levels of free SH groups across all formulations compared to their corresponding meat analogues post-extrusion. This consistent reduction in SH groups in extrudates was observed in previous studies as well, indicating that a portion of the sulfhydryl groups undergo oxidation to form disulfide bonds, contributing to the crosslinking of protein molecules.[70,71] Among the extrudates, the highest free SH content was observed in the 20% DCM meat analogue, followed by the 10% DCM meat analogue and control sample. On the other hand, 30–50% DCM samples showed consistently lower SH values likely due to the dilution effect, where increasing DCM reduces the overall concentration of reactive sulfhydryl groups due to the low protein content in DCM. The addition of TGase did not significantly alter the free SH content compared to the untreated DCM samples. This indicates that TGase likely facilitated crosslinking by catalyzing the acyl transfer reaction between lysine and glutamine residues rather than affecting thiol oxidation.[20]

Disulfide bonds are formed during the extrusion as a result of oxidative reactions of sulfhydryl groups, which were exposed due to mechanical shear forces during extrusion.[72] As depicted in (Fig. 6b), DCM substitution up to 30% enhanced S–S bond formation, likely due to the optimal balance between protein concentration and unfolding. Previous studies have also indicated that addition of carbohydrates can enhance S–S bond formation through oxidative interactions, resulting in a denser protein network structure.[7]

However, beyond 30% DCM, S–S bond content declined, which may be attributed to the reduced availability of cysteine residues from excessive DCM incorporation, thereby limiting crosslinking capacity. The role of TGase in modulating disulfide linkages appears minimal, as its enzymatic activity is not directly involved with cysteine residues. Overall, these findings highlight that moderate incorporation of DCM (10–30%) promotes a favorable balance between protein unfolding and crosslinking, essential for achieving the desired fibrous structure in meat analogues.

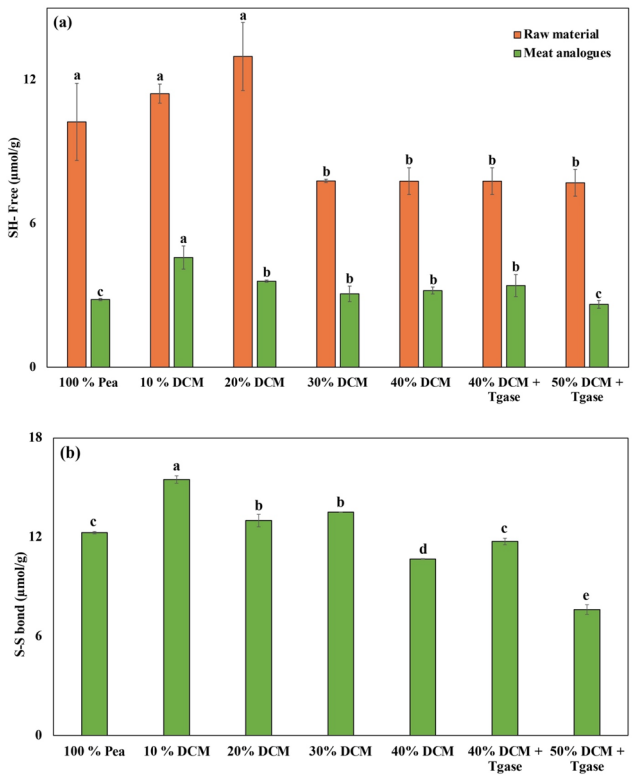

Fig. 6 (a) The free sulfhydryl (–SH) group content in raw materials (shown in brick red) and in their corresponding high-moisture extruded meat analogues (shown in green). (b) The disulfide bond (–S–S–) content in extruded meat analogues formulated with different levels of DCM substitution, with and without TGase. Values are expressed as mean ± SD ($n = 3$). Different superscript letters within the same sample type indicate significant differences ($p < 0.05$).

3.10 SEM

The impact of DCM on the microstructure of the extruded HMMA was evaluated using scanning electron microscopy (SEM) (Fig. 7). The control sample (100% pea protein) exhibited a relatively compact and layered structure, characteristic of fibrous meat analogues. However, the fiber alignment appeared limited, and the surface was smoother, suggesting a dense yet poorly oriented matrix. The addition of 10–20% DCM significantly enhanced the structural organization of the extrudates. SEM images revealed well-aligned, continuous fibrillar networks with minimal voids or cracks at 10% DCM, while 20% DCM maintained a cohesive matrix with only slight reductions in uniformity. This suggests that DCM incorporation up to 20% supports an optimal balance between protein content and dietary fiber, facilitating effective protein unfolding and intermolecular interactions. Similar improvements in structural integrity were reported in HMMAs containing curdlan and β-glucan, where enhanced hydrogen bonding and disulfide bond formation led to denser and smoother textures.[8,9,24]

However, as the DCM substitution increased beyond 20%, the fibrousness of the extrudates began to decline. At 30% DCM, although the fibrous texture remained visible macroscopically, SEM images showed fragmented fibrillar networks with emerging micro-tears. This structural disruption became more evident at 40% DCM, where the SEM images exhibited a rough, disordered matrix with prominent surface cracks and poor alignment. The corresponding macro photographs also reflected this breakdown, revealing a coarse, crumbly texture lacking distinct fibrous layers. The observed texture deterioration is likely due to excessive fiber and reduced protein content in DCM, which may impede the formation of a cohesive and well-aligned protein network during extrusion. Interestingly,

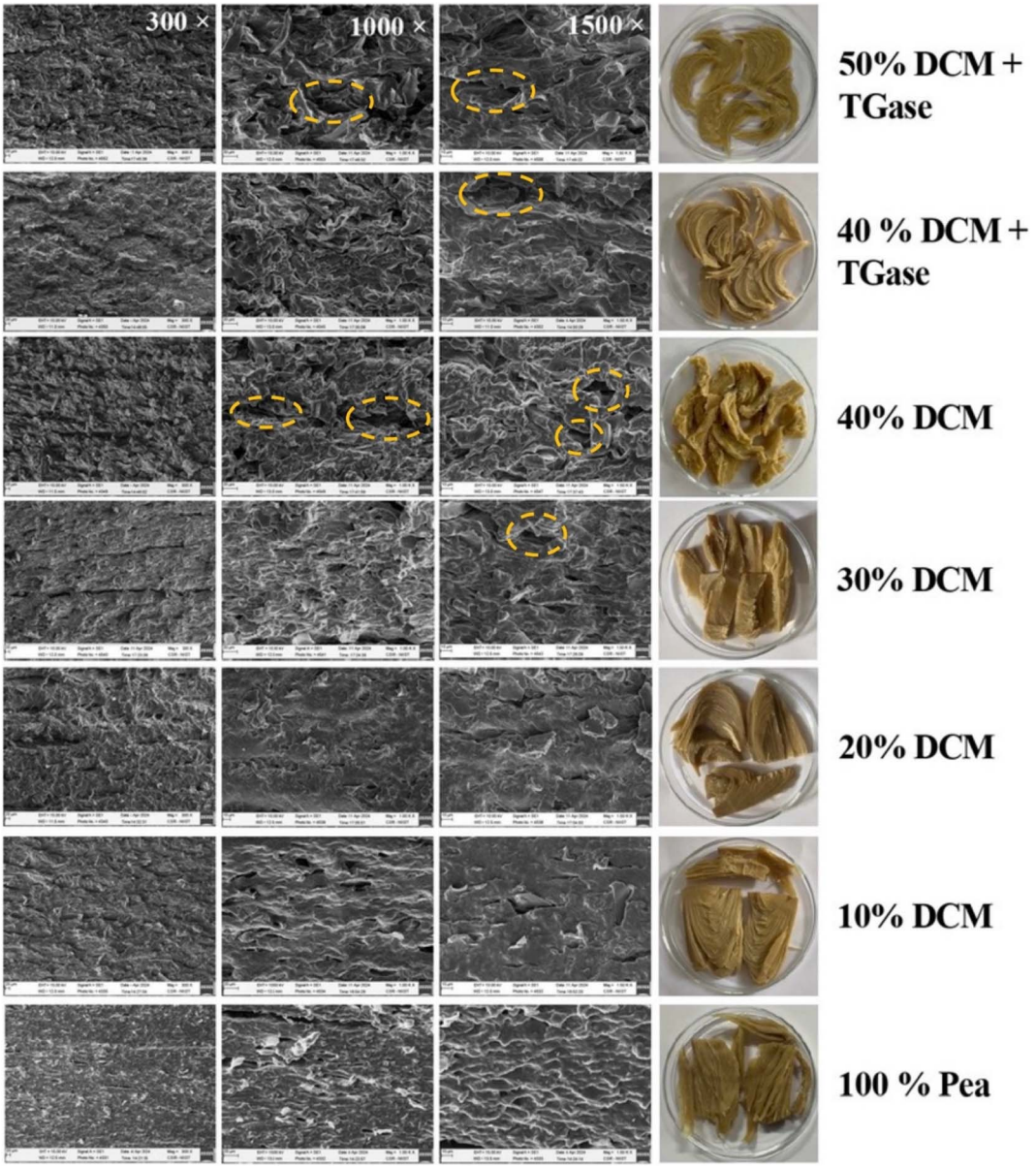

Fig. 7 Scanning electron microscopy (SEM) micrographs showing the microstructure of meat analogue extrudates. All samples were freeze-dried, gold-coated, and imaged at a magnification of 300×, 500×, and 1500×.

the addition of 0.25% TGase at 40% DCM improved the compactness of the structure, as evidenced by fewer micro-cracks and a denser surface morphology in SEM images. The corresponding macrostructure appeared slightly smoother and less fragmented than its untreated counterpart, suggesting that TGase-mediated crosslinking partially restored the fibrousness of HMMAs, promoting bonding between DCM and pea protein. The positive impact of TGase in improving extrudate compactness has also been reported previously.[73] In the case of 50% DCM + TGase, the macro images showed a dense and compact structure, but SEM revealed a comparatively disordered morphology with aggregation and minimal alignment when compared to other samples. Overall, the SEM analysis indicates that moderate DCM substitution (10–30%) supports fibrous structure formation by enhancing matrix density without compromising protein alignment. Furthermore, TGase demonstrated potential to mitigate structural degradation at higher levels of DCM incorporation, beyond 30% substitution.

4. Conclusion

This study critically evaluated the feasibility of DCM as an upcycled byproduct from the coconut industry, for the production of HMMAs. DCM contains 24.68% protein and 52.29% TDF, both of which played a crucial role in improving the macromolecular and nutritional characteristics of the DCM-incorporated HMMA. The findings demonstrate that DCM is a sustainable, clean-label and functional ingredient with strong

potential as a PPC substitute in HMMA formulations. Incorporation of DCM at 10–20% (w/w) significantly improved fibrous alignment, structural compactness, and protein crosslinking, resulting in extrudates with superior textural properties. However, substitution levels beyond 30% compromised HMMA matrix integrity, likely due to insufficient protein content required for effective anisotropic fiber network formation. The addition of TGase at higher DCM levels successfully restored crosslinking density and improved matrix compactness, highlighting its synergistic role in high-fiber and protein systems. Overall, the outcomes of this study highlight two important observations: first, the valorization of an agro-industrial byproduct, aligning with clean-label and circular economy principles, and second, the nutritional improvement of HMMAs through dietary fiber incorporation in the form of DCM. Thus, moderate incorporation of DCM presents a promising approach for developing sustainable meat analogues that meet consumer expectations for texture, nutrition, and clean label requirements. DCM can be further valorized into high-value, protein- and fibre-rich technofunctional food ingredients to develop a sustainable food system.

Author contributions

A. A. Anoop: writing – original draft, review and editing, and formal analysis. Anjali Sunil Ojha: formal analysis and writing – original draft. K. V. Ragavan: conceptualization, supervision, and writing – original draft, review, and editing.

Conflicts of interest

The authors declare no conflicts of interest.

Data availability

The authors confirm that all relevant data supporting the findings of this study are included in the article. Raw data files are available from the authors and can be provided upon reasonable request.

Acknowledgements

Anoop thanks the University Grants Commission for providing a Senior Research Fellowship (File No. F.15-6(DEC.2019)/2020(NET)) to pursue doctoral work at CSIR-NIIST. The authors thank the Director of CSIR-NIIST for providing necessary infrastructure and encouragement to conduct this research work.

References

1 United Nations, *World Population Prospects 2022: Summary of Results*, 2022.
2 F. Michel, C. Hartmann and M. Siegrist, *Food Qual. Prefer.*, 2021, **87**, 104063.
3 J. Poore and T. Nemecek, *Science*, 2018, **360**, 987–992.
4 Allied Market Research, *Vegan Food Market Size, Share, Competitive Landscape and Trend Analysis Report, by Product Type and Distribution Channel : Global Opportunity Analysis and Industry Forecast 2021-2030*, 2021.
5 B. L. Dekkers, R. M. Boom and A. J. Van Der Goot, *Trends Food Sci. Technol.*, 2018, **81**, 25–36.
6 T. P. Trinidad, A. C. Mallillin, D. H. Valdez, A. S. Loyola, F. C. Askali-Mercado, J. C. Castillo, R. R. Encabo, D. B. Masa, A. S. Maglaya and M. T. Chua, *Innovative Food Sci. Emerging Technol.*, 2006, **7**, 309–317.
7 T. Xiao, X. Su, R. Jiang, H. Zhou and T. Xie, *LWT–Food Sci. Technol.*, 2023, **179**, 114660.
8 W. Yang, C. Deng, L. Xu, W. Jin, J. Zeng, B. Li and Y. Gao, *Food Res. Int.*, 2020, **132**, 109111.
9 X. Ye, X. Su, T. Xiao, F. Lu and T. Xie, *Food Chem.*, 2024, **441**, 138329.
10 A. Marczak and A. C. Mendes, *Foods*, 2024, **13**, 1952.
11 J. Zhang, T. Li, Q. Chen, H. Liu, D. L. Kaplan and Q. Wang, *Food Res. Int.*, 2023, **166**, 112623.
12 M. Motoki and K. Seguro, *Trends Food Sci. Technol.*, 1998, **9**, 204–210.
13 A. Zimoch-Korzycka, A. Krawczyk, Ż. Król-Kilińska, D. Kulig, Ł. Bobak and A. Jarmoluk, *Foods*, 2024, **13**, 4085.
14 I. Zahari, F. Ferawati, J. K. Purhagen, M. Rayner, C. Ahlström, A. Helstad and K. Östbring, *Foods*, 2021, **10**, 2397.
15 K. Jakobson, A. Kaleda, K. Adra, M.-L. Tammik, H. Vaikma, T. Kriščiunaite and R. Vilu, *Foods*, 2023, **12**, 2805.
16 S. Branch and S. Maria, *Int. Food Res. J.*, 2017, **24**, 1595–1605.
17 S. Bhusari, K. Muzaffar and P. Kumar, *Powder Technol.*, 2014, **266**, 354–364.
18 S. Faisal, J. Zhang, S. Meng, A. Shi, L. Li, Q. Wang, S. J. Maleki and B. Adhikari, *Food Chem.*, 2022, **385**, 132569.
19 S. Xia, Y. Xue, C. Xue, X. Jiang and J. Li, *Lwt*, 2022, **154**, 112756.
20 Z. Sun, W. Zhang, F. Zhang, I. Chiu, D. Li, X. Wu, T. Yang, Y. Gao and H. Zheng, *Food Res. Int.*, 2025, **208**, 116229.
21 B. V. McCleary, J. W. De Vries, J. I. Rader, G. Cohen, L. Prosky, D. C. Mugford, M. Champ, K. Okuma, L. Abercrombie, N. Ames, T. Bajoras, S. Bhandari, G. Burkhardt, M. Camire, G. Cohen, S. Cui, M. P. Dougherty, S. Erhardt, A. Evans, M. Grutters, M. Hutton-Okpalaeke, S. Illaens, K. Kanaya, A. Kohn, E. Konings, G. Lai, T. Lee, M. Marshak, U. Neese, T. Nishibata, A. Santi, D. Saylor, M. Steegmans, H. Themeier, A. Thomsen, A. Tervila-Wilo, R. Walker and C. Wang, *J. AOAC Int.*, 2010, **93**, 221–233.
22 B. V. McCleary, J. W. DeVries, J. I. Rader, G. Cohen, L. Prosky, D. C. Mugford, M. Champ and K. Okuma, *J. AOAC Int.*, 2012, **95**, 824–844.
23 C. Li, H. Xue, Z. Chen, Q. Ding and X. Wang, *Food Res. Int.*, 2014, **57**, 1–7.
24 K. Zhang, D. Li, I. Chiu, X. Guo, Z. Sun, X. Wu, D. Liu, H. Chen, T. Yang, Y. Gao and H. Zheng, *Food Hydrocolloids*, 2025, **162**, 110998.
25 R. Xiao, J. Flory, S. Alavi and Y. Li, *Food Hydrocolloids*, 2025, **163**, 111119.

26 B. Chambal, B. Bergenståhl and P. Dejmek, *Food Res. Int.*, 2012, **47**, 146–151.
27 Y. Chen, T. Li, L. Jiang, Z. Huang, W. Zhang and Y. Luo, *Int. J. Biol. Macromol.*, 2024, **280**, 135905.
28 P. Rodsamran and R. Sothornvit, *Food Chem.*, 2018, **241**, 364–371.
29 A. S. Beniwal, J. Singh, L. Kaur, A. Hardacre and H. Singh, *Compr. Rev. Food Sci. Food Saf.*, 2021, **20**, 1221–1249.
30 O. G. Jones, *Curr. Opin. Food Sci.*, 2016, **7**, 7–13.
31 C. Köhn, A. Fontoura, A. Kempka, I. Demiate, E. Kubota and R. Prestes, *Int. Food Res. J.*, 2015, 356–362.
32 H. Fuhrmeister and F. Meuser, *J. Food Eng.*, 2003, **56**, 119–129.
33 A. Fernández-Quintela, M. Macarulla, A. Del Barrio and J. Martínez, *Plant Foods Hum. Nutr.*, 1997, **51**, 331–341.
34 H. Shakeela, K. Mohan and N. P, *Sustainable Food Technol.*, 2024, **2**, 497–505.
35 C. E. Wagner, J. K. Richter, M. Ikuse and G. M. Ganjyal, *J. Food Sci.*, 2024, **89**, 6098–6112.
36 K. Kyriakopoulou, J. K. Keppler and A. J. Van Der Goot, *Foods*, 2021, **10**, 600.
37 J. Fernández-López, E. Sendra, E. Sayas-Barberá, C. Navarro and J. A. Pérez-Alvarez, *Meat Sci.*, 2008, **80**, 410–417.
38 M. L. García, R. Dominguez, M. D. Galvez, C. Casas and M. D. Selgas, *Meat Sci.*, 2002, **60**, 227–236.
39 M. Benković, A. Jurinjak Tušek, T. Sokač Cvetnić, T. Jurina, D. Valinger and J. Gajdoš Kljusurić, *Gels*, 2023, **9**, 921.
40 E. Schmid, A. Farahnaky, B. Adhikari and P. J. Torley, *Compr. Rev. Food Sci. Food Saf.*, 2022, **21**, 4573–4609.
41 S. Chanarat and S. Benjakul, *Food Hydrocolloids*, 2013, **30**, 704–711.
42 X. Luo, J. Li, W. Yan, R. Liu, T. Yin, J. You, H. Du, S. Xiong and Y. Hu, *Int. J. Biol. Macromol.*, 2020, **160**, 642–651.
43 E. J. Ramírez-Rivera, B. Hernández-Santos, J. M. Juárez-Barrientos, J. G. Torruco-Uco, E. Ramírez-Figueroa and J. Rodríguez-Miranda, *J. Food Process. Preserv.*, 2021, **45**, e15499.
44 N. D. Turner and J. R. Lupton, *Adv. Nutr.*, 2011, **2**, 151–152.
45 T. P. Trinidad, A. C. Mallillin, D. H. Valdez, A. S. Loyola, F. C. Askali-Mercado, J. C. Castillo, R. R. Encabo, D. B. Masa, A. S. Maglaya and M. T. Chua, *Innovative Food Sci. Emerging Technol.*, 2006, **7**, 309–317.
46 K. Raghavarao, S. Raghavendra and N. Rastogi, *Indian Coconut J.*, 2008, 2–7.
47 H. H. Salama, S. M. Abdelhamid and N. S. Abd-Rabou, *Curr. Bioact. Compd.*, 2020, **16**, 661–670.
48 United States Department of Agriculture (USDA), *Coconut Products—Food Composition Database*, 2019.
49 N. Seetapan, N. Limparyoon, P. Raksa, C. Gamonpilas and P. Methacanon, *Int. J. Food Sci. Technol.*, 2024, **59**, 7619–7628.
50 Food Safety and Standards Authority of India (FSSAI), *Food Safety and Standards (Advertising and Claims) Regulations, 2018*, New Delhi, India, 2018.
51 A. A. M. Andersson, R. Andersson, A. Jonsäll, J. Andersson and H. Fredriksson, *J. Food Sci.*, 2017, **82**, 1344–1350.
52 F. Esposito, G. Arlotti, A. Maria Bonifati, A. Napolitano, D. Vitale and V. Fogliano, *Food Res. Int.*, 2005, **38**, 1167–1173.
53 A. Anoop, P. Ramees and K. Ragavan, *Sustainable Food Technol.*, 2025, 1164–1174.
54 X. D. Sun and S. D. Arntfield, *Food Hydrocolloids*, 2012, **28**, 325–332.
55 A. Turki, A. E. Oudiani, S. Msahli and F. Sakli, in *International Conference of Applied Research on Textile and Materials*, Springer, 2020, pp. 268–275.
56 B. Wang, H. Lu, H. Lou, D. R. Acharya, Y. Shi and Q. Chen, *Food Hydrocolloids*, 2024, **155**, 110190.
57 A. Rohman, Y. B. Che Man, A. Ismail and P. Hashim, *J. Am. Oil Chem. Soc.*, 2010, **87**, 601–606.
58 N. Vlachos, Y. Skopelitis, M. Psaroudaki, V. Konstantinidou, A. Chatzilazarou and E. Tegou, *Anal. Chim. Acta*, 2006, **573**, 459–465.
59 M. Di Foggia, P. Taddei, A. Torreggiani, M. Dettin and A. Tinti, *Proteomics Res. J.*, 2011, **2**, 231.
60 Z. Ganim, H. S. Chung, A. W. Smith, L. P. DeFlores, K. C. Jones and A. Tokmakoff, *Acc. Chem. Res.*, 2008, **41**, 432–441.
61 S. Chanarat and S. Benjakul, *Food Hydrocolloids*, 2013, **30**, 704–711.
62 Z. Sun, W. Zhang, F. Zhang, I. Chiu, D. Li, X. Wu, T. Yang, Y. Gao and H. Zheng, *Food Res. Int.*, 2025, **208**, 116229.
63 R. Gunarathne, N. Marikkar, E. Mendis, C. Yalegama, L. Jayasinghe and S. Ulpathakumbura, *J. Food Chem. Nanotechnol.*, 2022, **8**, 69–75.
64 V. Sante-Lhoutellier, L. Aubry and P. Gatellier, *J. Agric. Food Chem.*, 2007, **55**, 5343–5348.
65 W. Jiang, J. Feng, X. Yang and L. Li, *LWT–Food Sci. Technol.*, 2024, **194**, 115823.
66 J. Li and L. Li, *Food Chem.*, 2023, **429**, 136787.
67 N. Nikmaram, S. Y. Leong, M. Koubaa, Z. Zhu, F. J. Barba, R. Greiner, I. Oey and S. Roohinejad, *Food Control*, 2017, **79**, 62–73.
68 Y. Li, Y. Zheng, Y. Zhang, J. Xu and G. Gao, *Molecules*, 2018, **23**, 707.
69 J. Qin, Y. Zhao, J. Zhou, G. Zhang, J. Li and X. Liu, *Front. Nutr.*, 2022, **9**, 970010.
70 Y. Chen, Y. Liang, F. Jia, D. Chen, X. Zhang, Q. Wang and J. Wang, *Int. J. Biol. Macromol.*, 2021, **166**, 1377–1386.
71 B. Mao, J. Singh, S. Hodgkinson, M. Farouk and L. Kaur, *Food Hydrocolloids*, 2024, **147**, 109341.
72 O. K. Mosibo, G. Ferrentino, M. R. Alam, K. Morozova and M. Scampicchio, *Crit. Rev. Food Sci. Nutr.*, 2022, **62**, 2526–2547.
73 J. Zhang, Q. Chen, L. Liu, Y. Zhang, N. He and Q. Wang, *Food Hydrocolloids*, 2021, **112**, 106346.

